Optimal Control via Integrating the Dynamics of Magnetorheological Dampers and Structures

Fayezioghani, A.[1] and Moharrami H.[2*]

[1] M.Sc, Department of Structural Engineering, Faculty of Civil and Environmental Engineering, Tarbiat Modares University, Iran.

[2] Associate Professor, Department of Structural Engineering, Faculty of Civil and Environmental Engineering, Tarbiat Modares University, Iran.

Abstract: Magnetorheological (MR) dampers have the advantage of being tuned by low voltages. This has attracted many researchers to develop semi-active control of structures in theory and practice. Most of the control strategies first obtain the desired forces of dampers without taking their dynamics into consideration and then determine the input voltages according to those forces. As a result, these strategies may face situations where the desired forces cannot be produced by the dampers. In this article, by integrating the equations of the dynamics of MR dampers and the structural motion, and solving them in one set, a more concise semi-active optimal control strategy is presented, so as to bypass the aforementioned drawback. Next, a strong database that can be utilized to form a controller for more realistic implementations is produced. As an illustrative example, the optimal voltages of the dampers of a six-storey shear building are obtained under the scaled El-Centro earthquake and used to train a set of integrated analysis-adaptive neuro-fuzzy inference systems (ANFISs) as a controller. Results show that the overall performance of the proposed strategy is higher than most of the other conventional methods.

Keywords: ANFIS, Earthquake excitation, MR damper, Optimal control, Semi-active control.

INTRODUCTION

Protection of structures in terms of structural integrity and service ability against various lateral loads such as earthquake and strong winds is now moving from heavy reliance on the inelastic deformation of the structure to dissipation of energy, by means of energy-dissipative equipment. This requires the development of various structural passive, active, semi-active, and hybrid control devices for the mitigation of undesired responses against dynamic loads.

The magnetorheological (MR) damper, which is one of the most effective, high-capacity, semi-active control devices, inputs no energy into the structure and is adaptable over a wide range of loading conditions. This property makes it strongly suitable for structural control, in practice. They are not only more energy-efficient than active devices, but also more effective in absorbing seismic energy than passive ones.

Dyke et al. (1997) presented a comparative study on semi-active control strategies for the MR damper. Zhang et al. (1999) used a linear quadratic Gaussian/loop transfer recovery (LQG/LTR) active control strategy, based on acceleration feedback in

∗ Corresponding author Email: hamid@modares.ac.ir

conjunction with an MR damper, to reduce the responses of a tall structure excited by wind. Bani-Hani et al. (1999a, b) developed and designed three active controllers: Two neuro-controllers, one with a single sensor feedback and the other with three sensor feedbacks, and one optimal controller with acceleration feedback. Xu et al. (2000) proposed two optimal displacement control strategies, for the semi-active control of the seismic response of frame structures, using MR and *electrorheological (*ER) dampers. The early employment of fuzzy logic in control of a nonlinear structure may be traced back to Casciati et al. (1996). Schurter et al. (2001), discussed the motivations of using a fuzzy logic controller and the guidelines to design an ANFIS. Many researchers have utilized fuzzy logic as a controller whose rule base and parameters of membership function are determined by a classic or heuristic optimization algorithm, such as, the gradient descent method or genetic algorithm, respectively. Chase et al. (2004) developed a quadratic output regulator that minimizes the total structural energy and tested this regulator on a real, non-linear, semi-active structural control case study. K-Karamodin et al. (2010) employed a semi-active neuro-predictive controller for a nonlinear benchmark building. In the study by Shirazi et al. (2012), two types of controllers were considered. First, an H_∞ inverse control, based on the mixed-sensitivity design; and second, a dynamic output-feedback linear parameter-varying (LPV controller). There are some other references that may also be referred to as studies on control by fuzzy logic and/or neural networks (Yao, et al., 2013; Ghaffarzadeh, 2013; Kim, 2014; Yan et al., 2006; Xu et al., 2008; Faruque et al., 2009; and Das et al., 2011).

The strategies applied in the semi-active control of structures can be divided into two categories, according to whether they directly consider the dynamics of the controller device or not. In this article, a semi-active optimal control strategy that explicitly integrates the dynamics of MR dampers and the structural linear equation of motion is presented. In this control strategy, first, an optimization problem is established, in which a multi-objective functional integrates several structural quantities of interest, and the Bouc-Wen model of the MR dampers and the linear equation of motion of the structure under earthquake excitation comprise its constraints. An algorithm based on the "Steepest Descent" concept is used to find the optimal time histories of voltages that minimize the objective functional of the problem for the specified earthquakes. As an illustrative example, a six-storey shear building, presented in Jansen et al. (2000), is used, and the optimal voltages of its dampers are obtained under the scaled El-Centro earthquake. Next, using the optimal solutions, a set of integrated ANFISs is trained as a controller. Finally, the proposed strategy is compared to several conventional control methods as well as passive-on and passive-off.

MATERIALS AND METHODS

Magnetorheological Model

To accurately predict the behavior of the control system, the control devices should be modeled adequately. A simple mechanical model shown in Figure 1 was developed to precisely predict the behavior of the MR damper over a wide range of inputs. While there are some sophisticated models for behavior of MR dampers, (e.g., see Liem et al., 2015), the MR damper model used in this study is the prototype one modeled by Dyke et al. (1996).

The governing equations that predict the force of the MR dampers are as follows:

$$f_{damper} = c_0 \dot{x} + \alpha z \tag{1a}$$

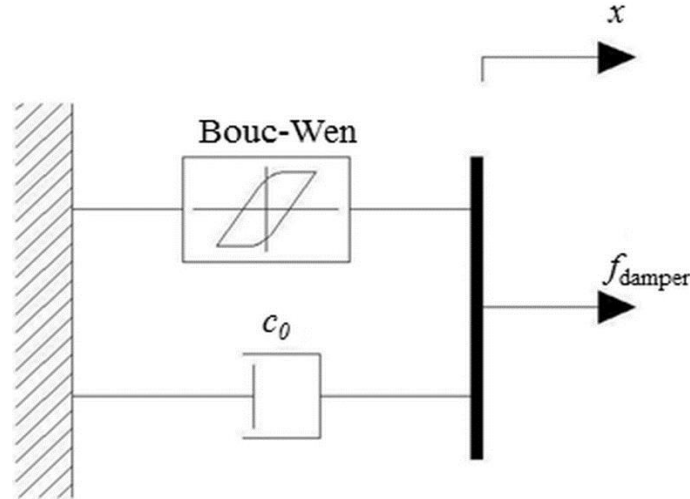$$\dot{z} = -\gamma |\dot{x}| z |z|^{N-1} - \beta \dot{x} |z|^N + A\dot{x} \tag{1b}$$

Fig. 1. Mechanical model of the MR damper

where f_{damper}: is the force generated by the damper, $\dot{x}$: is the relative velocity between the ends of the damper, and z: is the evolutionary variable that accounts for the history dependence of the response. The model parameters that depend on the real voltage u are defined by the following equations:

$$c_0 = c_{0a} + c_{0b} u \quad , \quad \alpha = \alpha_a + \alpha_b u \qquad (1c)$$

where u: is obtained as the output of the first order filter.

$$\dot{u} = -\eta(u - V) \qquad (1d)$$

where V: is the voltage applied to the damper. The dynamics involved in the MR fluid reaching rheological equilibrium are accounted for through a first order filter, Eq. (1d). In Eqs. (1b) to (1d) the parameters $\gamma, N, \beta, A, c_{0a}, c_{0b}, \alpha_{0a}, \alpha_{0b}$ and η depend on the characteristics of the damper.

Equation of Motion

Assume a shear building that has MR dampers installed to prevent damage from severe earthquake effects. The general equation of motion of the main structural system is defined in Eq. (2):

$$\mathbf{K}_S \mathbf{v} + \mathbf{C}_S \dot{\mathbf{v}} + \mathbf{M}_S \ddot{\mathbf{v}} = -\mathbf{M}_S \mathbf{1} \ddot{v}_g \qquad (2)$$

where $\mathbf{M}_s$, $\mathbf{K}_s$, and $\mathbf{C}_s$: represent the $n \times n$ seismic mass, structural stiffness, and inherent structural damping matrices, respectively; $\mathbf{v}, \dot{\mathbf{v}}$ and $\ddot{\mathbf{v}}$: are the floor displacement, velocity and acceleration vectors, respectively; $\ddot{v}_g$: is the ground acceleration, $\mathbf{1}$: is an $n \times 1$ unit vector of seismic load distribution, and n: is the number of storeys. The damping matrix can be constructed as defined in Eq. (3) (Clough et al., 2003):

$$\mathbf{C}_S = \mathbf{M}_S \left(\sum_{i=1}^{n} \frac{2 \xi_i \omega_i}{\boldsymbol{\varphi}_i^T \mathbf{M}_S \boldsymbol{\varphi}_i} \boldsymbol{\varphi}_i \boldsymbol{\varphi}_i^T \right) \mathbf{M}_S \qquad (3)$$

where ξ_i, ω_i^2 and $\boldsymbol{\varphi}_i$: are the damping coefficient, eigen value, and eigen vector relating to the ith mode shape, respectively.

To analyze the structure equipped with MR dampers, in the conventional methods, $\mathbf{f}_d$, the vector of the MR dampers' forces in Eq. (4a) given below is found by the solution of an optimization problem; then the voltages corresponding to $\mathbf{f}_d$ are found through a control law corresponding to various algorithms, such as, the Lyapunov Stability Theory, Decentralized Bang-Bang Control, Clipped-Optimal Control, Modulated Homogeneous Friction, and so on. However, in this article, and the proposed algorithm the equations of dynamic behavior of the MR dampers (Eqs. (4b) to (4d)) are added

to the linear equation of motion of the structure and then solved simultaneously. As a result, the voltages corresponding to the $\mathbf{f}_d$ are obtained directly in a more realistic manner, as follows;

$$\mathbf{K}_S\,\mathbf{v} + \mathbf{C}_S\,\dot{\mathbf{v}} + \mathbf{M}_S\,\ddot{\mathbf{v}} + \mathbf{D}\mathbf{f}_d = -\mathbf{M}_S\,\mathbf{1}\ddot{v}_g \quad (4a)$$

$$f_{dj} = (c_{0aj} + c_{0bj}u_j)\dot{x}_j + (\alpha_{aj} + \alpha_{bj}u_j)z_j$$
$$, j = 1 \sim n_d \quad (4b)$$

$$\dot{z}_j = -\gamma_j\left|\dot{x}_j\right|z_j\left|z_j\right|^{N_j-1} - \beta_j\dot{x}_j\left|z_j\right|^{N_j} + A_j\dot{x}_j \quad (4c)$$

$$\dot{u}_j = -\eta_j(u_j - V_j) \quad (4d)$$

where **D**: is the $n \times n_d$ matrix of location and the number of the dampers, n_d: is the number of storeys that have MR damper(s), and $f_{dj}, \dot{x}_j, z_j, u_j$, and V_j: are j^{th} component of the vectors $\mathbf{f}_d, \dot{\mathbf{x}}, \mathbf{z}, \mathbf{u}$, and $\mathbf{V}$, respectively. The relative velocity $\dot{\mathbf{x}}$ can be related to the floor velocity of the main structure by the following equation.

$$\dot{\mathbf{x}} = \mathbf{D}_d^T \mathbf{E}\dot{\mathbf{v}} \quad (5)$$

where $\mathbf{D}_d$: is the $n \times n_d$ matrix of only the location of dampers and matrix **E**: is defined as:

$$\mathbf{E} = \begin{cases} E_{i,i} = 1 & , i = 1 \sim n \\ E_{i,i-1} = -1 & , i = 2 \sim n \\ E_{i,j} = 0 & , i, j = 1 \sim n, j \neq i, i-1 \end{cases}$$

where $E_{i,j}$: represents the component located in the ith row and j^{th} column of matrix **E**.

Objective Function

To evaluate the control strategy, the following criteria, which are based on the responses of buildings, are used. All the criteria in Eqs. (6a) to (6c), except J_7 that is presented here for the numerical analyses, have been proposed by Ohtori et al. (2004).

$$J_1 = \frac{\max\limits_{t,i} \dfrac{\left|d_i^c(t)\right|}{h_i}}{\max\limits_{t,i} \dfrac{\left|d_i^u(t)\right|}{h_i}} \quad ,$$

$$J_2 = \frac{\max\limits_{t,i}\left|\ddot{v}_{ai}^c(t)\right|}{\max\limits_{t,i}\left|\ddot{v}_{ai}^u(t)\right|} \quad , \quad (6a)$$

$$J_3 = \frac{\max\limits_{t}\left|\sum\limits_i m_i\ddot{v}_{ai}^c(t)\right|}{\max\limits_{t}\left|\sum\limits_i m_i\ddot{v}_{ai}^u(t)\right|}$$

$$J_4 = \frac{\max\limits_{i} \dfrac{\left\|d_i^c(t)\right\|}{h_i}}{\max\limits_{i} \dfrac{\left\|d_i^u(t)\right\|}{h_i}} \quad ,$$

$$J_5 = \frac{\max\limits_{i}\left\|\ddot{v}_{ai}^c(t)\right\|}{\max\limits_{i}\left\|\ddot{v}_{ai}^u(t)\right\|} \quad , \quad (6b)$$

$$J_6 = \frac{\left\|\sum\limits_i m_i\ddot{v}_{ai}^c(t)\right\|}{\left\|\sum\limits_i m_i\ddot{v}_{ai}^u(t)\right\|}$$

$$J_7 = \frac{\max\limits_{t,i}\left|v_i^c(t)\right|}{\max\limits_{t,i}\left|v_i^u(t)\right|} \quad ,$$

$$J_8 = \frac{\max\limits_{t,i}\left|f_{di}(t)\right|}{W_T} \quad (6c)$$

where **d** and $\|.\|$: are defined as:

$$\mathbf{d}(t) = \mathbf{E}\mathbf{v}(t) \quad , \quad \|.\| = \sqrt{\frac{1}{t_f}\int_0^{t_f}(.)^2\,\mathrm{d}t}$$

where **d**: is the vector of relative displacement of the storeys, h_i: is the height of the ith storey; and m_i and $\ddot{v}_{ai} = \ddot{v}_i + \ddot{v}_g$: are the mass and absolute acceleration of the ith floor, respectively. W_T: is the total weight of the structure, t_f: is a sufficiently large time to allow for the response of the structure to attenuate. The

superscripts *c* and *u*: denote controlled and uncontrolled responses, respectively. To optimally control the structure under excitations, it is necessary to define an objective function. Here, an objective function composed of normalized effects of the time-averaged drifts of the floors, absolute accelerations of floors, base shear, and input voltages is suggested as follows:

$$J = \int_0^{t_f} \left(\mathbf{v}^T \mathbf{Q}'_v \mathbf{v} + \ddot{\mathbf{v}}_a^T \mathbf{Q}'_{\ddot{v}} \ddot{\mathbf{v}}_a + \ddot{\mathbf{v}}_a^T \mathbf{Q}'_{V_b} \ddot{\mathbf{v}}_a + \mathbf{V}^T \mathbf{R} \mathbf{V} \right) dt$$

(7)

where

$$\mathbf{Q}'_v = \frac{1}{n * t_f * \left(\max_{t,i} \dfrac{|d_i^u(t)|}{h_i} \right)^2} \mathbf{Q}_v,$$

$$\mathbf{Q}_v = \begin{cases} (Q_v)_{i,i} = \dfrac{1}{h_i^2} + \dfrac{1}{h_{i+1}^2}, \\ i = 1 \sim n \\ (Q_v)_{i+1,i} = (Q_v)_{i,i+1} = -\dfrac{1}{h_{i+1}^2}, \\ i = 1 \sim n-1 \\ (Q_v)_{i+j,i} = (Q_v)_{i,i+j} = 0, \\ 2 \le j \le n-i \end{cases}$$

$$\mathbf{Q}'_{\ddot{v}} = \frac{1}{n * t_f * \left(\max_{t,i} |\ddot{v}_{ai}^u(t)| \right)^2} \mathbf{Q}_{\ddot{v}},$$

$$\mathbf{Q}_{\ddot{v}} = \mathbf{I}_n$$

$$\mathbf{Q}'_{V_b} = \frac{1}{t_f * \left(\max_t \left| \sum_{i=1}^n m_i \ddot{v}_{ai}^u(t) \right| \right)^2} \mathbf{Q}_{V_b},$$

$$(Q_{V_b})_{i,j} = m_i * m_j,$$

$$i,j = 1 \sim n$$

where $\mathbf{Q}'_v, \mathbf{Q}'_{\ddot{v}}, \mathbf{Q}'_{V_b}$: are the normalized matrices for time-averaged drifts, absolute accelerations, and base shear, respectively. $\mathbf{I}_n$: is the identity matrix of dimension *n*, and $\mathbf{R}$: is the normalized weighting matrix, which shows the importance of dampers in comparison with each other. The

Lagrangian function for the optimization problem consisting of the objective function of Eq. (7) and constraints of Eqs. (4a) to (4d) can be constructed as follows:

$$J_a = \int_0^{t_f} \begin{pmatrix} \mathbf{v}^T \mathbf{Q}'_v \mathbf{v} + \ddot{\mathbf{v}}_a^T (\mathbf{Q}'_{\ddot{v}} + \mathbf{Q}'_{V_b}) \ddot{\mathbf{v}}_a + \\ \mathbf{V}^T \mathbf{R} \mathbf{V} + \\ \boldsymbol{\lambda}_1^T (\mathbf{K}''_S \mathbf{v} + \mathbf{C}''_S \dot{\mathbf{v}} + \mathbf{M}''_S \ddot{\mathbf{v}}_a) + \\ \displaystyle\sum_{i=1}^n \lambda_{1i} \sum_{j=1}^{n_d} D''_{ij}((c_{0aj} + c_{0bj}u_j)\dot{x}_j + \\ (\alpha_{aj} + \alpha_{bj}u_j)z_j) \\ \displaystyle\sum_{j=1}^{n_d} \lambda_{2j} (\dot{u}_j + \eta_j(u_j - V_j)) + \\ \displaystyle\sum_{j=1}^{n_d} \lambda_{3j} (\dot{z}_j + \gamma_j |\dot{x}_j| z_j |z_j|^{N_j - 1} + \\ \beta_j \dot{x}_j |z_j|^{N_j} - A_j \dot{x}_j) \end{pmatrix} dt$$

$$= \int_0^{t_f} F(\mathbf{v}(t), \dot{\mathbf{v}}(t), \ddot{\mathbf{v}}(t), \mathbf{V}(t), \mathbf{u}(t), \\ \mathbf{z}(t), \boldsymbol{\lambda}_1(t), \boldsymbol{\lambda}_2(t), \boldsymbol{\lambda}_3(t), t) dt$$

(8)

where $\boldsymbol{\lambda}_1, \boldsymbol{\lambda}_2$, and $\boldsymbol{\lambda}_3$: represent the Lagrange multipliers and $\mathbf{M}'', \mathbf{C}''_S, \mathbf{K}''_S$, and $\mathbf{D}''$: are the normalized matrices of the system as defined in the following:

$$\begin{bmatrix} \mathbf{M}''_S & \mathbf{C}''_S & \mathbf{K}''_S & \mathbf{D}'' \end{bmatrix} =$$

$$\frac{1}{F_I} \begin{bmatrix} \mathbf{M}_S & \mathbf{C}_S & \mathbf{K}_S & \mathbf{D} \end{bmatrix},$$

$$F_I = \max_{t,i} |\mathbf{M}_S \mathbf{1} \ddot{v}_g|$$

Optimal Control Method

In this study, the optimal control method proposed by Kirk (1970) is slightly modified and then employed to minimize the objective function defined in Eq. (8). For the following objective function and constraints

$$J = h(\mathbf{x}(t_f), t_f) +$$

$$\int_0^{t_f} g(\mathbf{x}(t), \dot{\mathbf{x}}(t), \mathbf{u}(t), t)) \, dt$$

(9a)

$$\dot{\mathbf{x}}(t) = \mathbf{a}(\mathbf{x}(t), \mathbf{u}(t), t)$$

(9b)

The augmented objective functional is

$$J_a = \int_0^{t_f} \left\{ g\left(\mathbf{x}(t),\dot{\mathbf{x}}(t),\mathbf{u}(t),t\right) + \left[\frac{\partial h(\mathbf{x}(t),t)}{\partial \mathbf{x}}\right]^T \dot{\mathbf{x}}(t) + \frac{\partial h(\mathbf{x}(t),t)}{\partial t} + \mathbf{p}^T(t)\left[\mathbf{a}(\mathbf{x}(t),\mathbf{u}(t),t) - \dot{\mathbf{x}}(t)\right] \right\} dt \quad (10)$$

where $\mathbf{x}(t)$: is the system state vector, $\mathbf{u}(t)$: is the system input vector, $h(.)$: is a function of final time and final state, and $\mathbf{a}(.)$ and $g(.)$: are functions of time, system state, and input; t_f: is the final time, and $\mathbf{p}(t)$: is the vector of the Lagrange multipliers. It is more convenient to use the Hamiltonian function defined in Eq. (11).

$$H\left(\mathbf{x}(t),\dot{\mathbf{x}}(t),\mathbf{u}(t),\mathbf{p}(t),t\right) =$$
$$g\left(\mathbf{x}(t),\dot{\mathbf{x}}(t),\mathbf{u}(t),t\right) + \quad (11)$$
$$\mathbf{p}^T(t)\left[\mathbf{a}(\mathbf{x}(t),\mathbf{u}(t),t)\right]$$

The necessary conditions to find the solution that minimizes Eq. (10) are:

$$\dot{\mathbf{x}}(t) = \frac{\partial H}{\partial \mathbf{p}(t)} \quad (12a)$$

$$\dot{\mathbf{p}}(t) = -\frac{\partial H}{\partial \mathbf{x}(t)} + \frac{d}{dt}\frac{\partial H}{\partial \dot{\mathbf{x}}(t)} \quad (12b)$$

$$0 = \frac{\partial H}{\partial \mathbf{u}(t)} \quad (12c)$$

The boundary conditions for the above differential equations can be obtained from Eq. (13).

$$\left[\begin{array}{c} \dfrac{\partial h(\mathbf{x}(t_f),t_f)}{\partial \mathbf{x}} + \\[2mm] \dfrac{\partial H(\mathbf{x}(t_f),\dot{\mathbf{x}}(t_f),\mathbf{u}(t_f),\mathbf{p}(t_f),t_f)}{\partial \dot{\mathbf{x}}} - \\[2mm] \mathbf{p}(t_f) \end{array}\right]^T \delta\mathbf{x}(t_f)$$
$$+ \left[\begin{array}{c} H(\mathbf{x}(t_f),\dot{\mathbf{x}}(t_f),\mathbf{u}(t_f), \\[1mm] \mathbf{p}(t_f),t_f) + \dfrac{\partial h(\mathbf{x}(t_f),t_f)}{\partial t} \end{array}\right] \delta t_f = 0$$

$$(13)$$

where $\delta\mathbf{x}(t_f)$ and δt_f: are the variations of final state and final time, respectively. If $\mathbf{x}(t_f)$ and/or t_f are specified, then $\delta\mathbf{x}(t_f)$ and/or δt_f will be zero; otherwise, to satisfy Eq. (13) for the trivial values, $\delta\mathbf{x}(t_f)$ and δt_f, their multipliers should be equal to zero.

According to Eqs. (12a) to (12c), the following nonlinear ordinary differential equations that are derived from Eq. (8) should be simultaneously solved.

$$\frac{\delta J_a}{\delta \boldsymbol{\lambda}_2} = 0 \Rightarrow \frac{\partial F}{\partial \boldsymbol{\lambda}_2} = \dot{u}_j + \eta_j(u_j - V_j) = 0 \,, \ j = 1 \sim n_d \quad (14a)$$

$$\frac{\delta J_a}{\delta \boldsymbol{\lambda}_1} = 0 \Rightarrow \frac{\partial F}{\partial \boldsymbol{\lambda}_1} = \mathbf{K}_S''\mathbf{v} + \mathbf{C}_S''\dot{\mathbf{v}} + \mathbf{M}_S''\ddot{\mathbf{v}} + \mathbf{D}''\left(\text{diag}[\mathbf{c}_{0a} + \mathbf{c}_{0b}:\mathbf{u}]\dot{\mathbf{x}} + \text{diag}[\boldsymbol{\alpha}_a + \boldsymbol{\alpha}_b:\mathbf{u}]\mathbf{z}\right) + \mathbf{M}_S''\mathbf{1}\ddot{v}_g = 0 \quad (14b)$$

$$\frac{\delta J_a}{\delta \boldsymbol{\lambda}_3} = 0 \Rightarrow \frac{\partial F}{\partial \boldsymbol{\lambda}_3} = \dot{z}_j + \gamma_j\left|\dot{x}_j\right|z_j\left|z_j\right|^{N_j-1} + \beta_j\dot{x}_j\left|z_j\right|^{N_j} - A_j\dot{x}_j = 0\,, \ j = 1 \sim n_d \quad (14c)$$

$$\frac{\delta J_a}{\delta \mathbf{v}} = 0 \Rightarrow \frac{\partial F}{\partial \mathbf{v}} - \frac{d}{dt}\frac{\partial F}{\partial \dot{\mathbf{v}}} + \frac{d^2}{dt^2}\frac{\partial F}{\partial \ddot{\mathbf{v}}} =$$
$$+\left(\mathbf{K}_S'' - \mathbf{E}^T\mathbf{D}_d\,\text{diag}[\mathbf{c}_{0b}:\dot{\mathbf{u}}]\,\mathbf{D}''^T\right)\boldsymbol{\lambda}_1 - \left(\mathbf{C}_S'' + \mathbf{E}^T\mathbf{D}_d\,\text{diag}[\mathbf{c}_{0a} + \mathbf{c}_{0b}:\mathbf{u}]\,\mathbf{D}''^T\right)\dot{\boldsymbol{\lambda}}_1 + \left(\mathbf{M}_S''\right)\ddot{\boldsymbol{\lambda}}_1$$
$$-\left(\mathbf{E}^T\mathbf{D}_d\,\text{diag}[\mathbf{N}:(\boldsymbol{\gamma}:\text{sign}(\dot{\mathbf{x}}) + \boldsymbol{\beta}:\text{sign}(\mathbf{z})):\left|\mathbf{z}\right|^{:N-1}:\dot{\mathbf{z}}]\right)\boldsymbol{\lambda}_3 - \left(\mathbf{E}^T\mathbf{D}_d\,\text{diag}[(\boldsymbol{\gamma}:\text{sign}(\dot{\mathbf{x}}):\text{sign}(\mathbf{z}) + \boldsymbol{\beta}):\left|\mathbf{z}\right|^{:N} - \mathbf{A}]\right)\dot{\boldsymbol{\lambda}}_3 \quad (14d)$$
$$+2\mathbf{Q}_v'\mathbf{v} + 2(\mathbf{Q}_{\dot{v}}' + \mathbf{Q}_{V_b}')(\ddot{\mathbf{v}} + \mathbf{1}\ddot{v}_g) = 0$$

$$\frac{\delta J_a}{\delta \mathbf{z}} = 0 \Rightarrow \frac{\partial F}{\partial \mathbf{z}} - \frac{\mathrm{d}}{\mathrm{d}t}\frac{\partial F}{\partial \dot{\mathbf{z}}} =$$

$$\left(\mathrm{diag}[\boldsymbol{\alpha}_a + \boldsymbol{\alpha}_b : \mathbf{u}] \, \mathbf{D}''^T\right)\boldsymbol{\lambda}_1 + \left(\mathrm{diag}[\mathbf{N}:(\boldsymbol{\gamma}:\mathrm{sign}(\dot{\mathbf{x}}) + \boldsymbol{\beta}:\mathrm{sign}(\mathbf{z})):|\mathbf{z}|^{:\mathbf{N}-1}:\dot{\mathbf{x}}]\right)\boldsymbol{\lambda}_3 - \dot{\boldsymbol{\lambda}}_3 = 0 \quad (14e)$$

$$\frac{\delta J_a}{\delta \mathbf{V}} = 0 \Rightarrow \frac{\partial F}{\partial \mathbf{V}} = 2\mathbf{RV} - \mathrm{diag}[\boldsymbol{\eta}]\boldsymbol{\lambda}_2 = 0 \quad (14f)$$

$$\frac{\delta J_a}{\delta \mathbf{u}} = 0 \Rightarrow \frac{\partial F}{\partial \mathbf{u}} - \frac{\mathrm{d}}{\mathrm{d}t}\frac{\partial F}{\partial \ddot{\mathbf{u}}} = \left(\mathrm{diag}[\mathbf{c}_{0b}:\dot{\mathbf{x}}+\boldsymbol{\alpha}_b:\mathbf{z}]\,\mathbf{D}''^T\right)\boldsymbol{\lambda}_1 + \mathrm{diag}[\boldsymbol{\eta}]\boldsymbol{\lambda}_2 - \dot{\boldsymbol{\lambda}}_2 = 0 \quad (14g)$$

where $\delta J_a/\delta \mathbf{X}(t)$: is the variation of J_a with respect to vector $\mathbf{X}(t)$, $\mathbf{X}:\mathbf{Y}$, and $\mathbf{X}^{:\mathbf{Y}}$, which show the point-wise product and point-wise power, respectively, diag[.]: is the diagonal matrix operator, and sign (.): is the sign function as below

$$(\mathbf{X}:\mathbf{Y})_i = X_i Y_i, (\mathbf{X}^{:\mathbf{Y}})_i =$$

$$X_i^{Y_i}, \mathrm{diag}[\mathbf{X}]_{i,j} = \begin{cases} X_i & ,i=j \\ 0 & ,i \neq j \end{cases},$$

$$\mathrm{sign}(x) = \begin{cases} +1 & ,x>0 \\ 0 & ,x=0 \\ -1 & ,x<0 \end{cases}$$

To determine the functions that minimize the objective function or solve Eqs. (14a) to (14g), a steepest descent algorithm is proposed. The following step by step algorithm describes the solution procedure:

1. Assume initial functions for the vector of real voltages $\mathbf{u}^k(t)$, $k=0$.

2. For $\mathbf{u}^k(t)$ to remain in its bounds, that is, $V_L \leq \mathbf{u}^k(t) \leq V_U$, replace $\mathbf{u}^k(t)$ with $B(\mathbf{u}^k(t); V_L, V_U)$ as defined in the following

$$B(\mathbf{u};V_L,V_U) = \begin{cases} V_L & ,\mathbf{u}<V_L \\ \mathbf{u} & ,V_L \leq \mathbf{u} \leq V_U \\ V_U & ,\mathbf{u}>V_U \end{cases}$$

3. Calculate $\mathbf{V}^k(t)$ from Eq. (14a)

4. Solve the differential Eqs. (14b) and (14c) with initial conditions $\mathbf{v}^k(0) = \dot{\mathbf{v}}^k(0) = 0$ and $\mathbf{z}^k(0)=0$ to obtain $\mathbf{v}^k(t)$ and $\mathbf{z}^k(t)$.

5. Solve the differential Eq. (14d) and Eq. (14e) with the terminal condition $\lambda_3^k(t_f)=0$, in addition to the following terminal conditions, to obtain $\lambda_1^k(t)$ and $\lambda_3^k(t)$.

$$\boldsymbol{\lambda}_1(t_f) = -2\mathbf{M}_S''^{-1}(\mathbf{Q}_{\ddot{v}}'+\mathbf{Q}_{V_b}')(\ddot{\mathbf{v}}(t_f)+$$
$$\mathbf{1}\ddot{v}_g(t_f))$$
$$\dot{\boldsymbol{\lambda}}_1(t_f) =$$
$$\mathbf{M}_S''^{-1}\begin{pmatrix} -2(\mathbf{Q}_{\ddot{v}}'+\mathbf{Q}_{V_b}')(\dddot{\mathbf{v}}(t_f)+\mathbf{1}\dddot{v}_g(t_f))+ \\ (\mathbf{C}_S''+\mathbf{E}^T\mathbf{D}_d \\ \mathrm{diag}[\mathbf{c}_{0a}+\mathbf{c}_{0b}:\mathbf{u}(t_f)]\mathbf{D}''^T)\boldsymbol{\lambda}_1(t_f) \end{pmatrix}$$

6. Calculate $\lambda_2^k(t)$ from Eq. (14f).

7. Calculate $\mathbf{g}^k = \left(\frac{\partial F}{\partial \mathbf{u}} - \frac{\mathrm{d}}{\mathrm{d}t}\frac{\partial F}{\partial \dot{\mathbf{u}}}\right)^k$ from Eq. (14g).

8. If the following stopping criterion, in which ε: is a desired convergence parameter, is satisfied, then the $\mathbf{V}^k(t)$: is the optimal voltage.

$$J^k - J^{k-1} \leq \varepsilon$$

Otherwise, search for $\alpha^k(t)$ in the following equation that minimizes J^{k+1}.

$$\mathbf{u}^{k+1}(t) = B\left(\mathbf{u}^k(t) - \alpha^k(t)\mathbf{g}^k; V_L, V_U\right)$$

$\alpha^k(t)$, is varied by a scalar parameter β in the following equation during an internal loop.

$$\alpha^{k,l+1}(t) = \alpha^{k,l}(t) + \beta^{k,l}(\mathbf{g}^k)^T\mathbf{g}^{k,l}$$

9. Replace k by $k+1$ and return to step 2.

The Proposed Control Strategy

To control the structure subjected to earthquake excitations, fast and accurate control commands should be given to the dampers. By including the equations of the dynamics of the MR dampers in the control strategy, the optimal voltages will theoretically be the most accurate commands that can be obtained for each given earthquake record. In addition, as fuzzy

inference systems and neural networks are fast and universal tools of approximation, the obtained optimal data can be used to train offline a set of ANFISs as an online controller. The controller can rapidly issue online nearly optimal voltage commands to the dampers during earthquakes. The accuracy of the outputs of the controller mainly depends on the number of inputs and the theoretical dependency of the outputs to the inputs.

In this study, a set of ANFISs have been trained, by absolute accelerations of floors, as the inputs, and optimal voltages, as the outputs. For any set of inputs, at any time step, there is a corresponding optimal voltage. Therefore, thousands of pairs of data (inputs and outputs) are obtained for training of the ANFISs for any given earthquake record. Because of the multi input/single output architecture of the ANFIS, individual ANFISs are trained separately for the damper(s) of each storey. Then all the ANFISs are integrated into a set of ANFISs that work in parallel.

RESULTS AND DISCUSSION

To demonstrate the effectiveness of the proposed semi-active control strategy, numerical simulations are carried out for a six-storey shear building example, with specifications applied in the study by Jansen et al. (2000). The building model has six 30-centimeter-height storeys each with 29.7 kNm^{-1} lateral stiffness and 22.7 kg seismic mass, and is equipped with two dampers in the first storey and two other dampers in the second storey. The capacity of each damper is 1.8% of the total mass of the building when applying the maximum voltage of 5 V. Also, the other parameters of the dampers are: c_{0a}=0.0064 N scm^{-1}, c_{0b}=0.0052 Nscm^{-1}. V^{-1}, α_a=8.66 Ncm^{-1}, α_b=8.66 Ncm^{-1}V^{-1}, β=300 cm^{-2}, γ=300cm^{-2}, A=120, N=2, and η=80 s^{-1}. The inherent damping matrix is constructed by using 0.5% damping for all modes. The ground excitations adopted in this study are Kobe,

El-Centro, Northridge, and Chi-Chi as shown in Figure 2.

The optimal time histories of voltages and the corresponding structural responses of the building under the first 20 seconds of the El-Centro acceleration, whose amplitude is scaled to 50% of its original record, are found by the aforementioned step by step algorithm. The convergence parameter is assumed to be ε =0.005 and the matrix **R** is experimentally set to $10^{-6} * \mathbf{I}_{n_d}$ so that the voltages are implicitly prevented from a long stay at their maximum level. After getting optimal data, the absolute accelerations of the fifth and sixth floors are used, to train the ANFISs, by using the fuzzy logic toolbox of MATLAB. In the architecture of ANFISs, the Sugeno fuzzy with nine generalized bell-shaped membership functions (gbellmfs) are employed for each input. Finally, the building that is equipped with dampers and the integrated controller is numerically simulated under the first 20 seconds of the El-Centro record that is scaled to 10% of its original amplitude. Obtaining the optimal voltages and training the two ANFISs take about 5 minutes and 10 seconds, respectively, on a personal computer with Intel 2.83GHz CPU. The required time for ANFISs to simultaneously command the dampers is approximately 0.17 milliseconds. If the input data and base acceleration are measured and sent to the controllers every 20 milliseconds, the remaining time for the dampers to respond will be more than 99% of this interval, which is enough to neglect the time delay of the semi-active control system. The time histories of the commanded voltages produced by ANFISs and the corresponding forces of dampers are shown in Figure 3. It can be seen from the voltages in Figure 3 that the controllers have been successful in reducing the peak structural responses, while holding the voltages at a low level, that is, the required instantaneous power is increased only

when necessary. Furthermore, the time histories of the forces produced by dampers show that the controllers have been moderately successful in preventing the ground seismic energy to be transferred to the upper unequipped storeys. The maximum forces for the first and the second dampers are 15.9 and 18.1 Newtons, respectively.
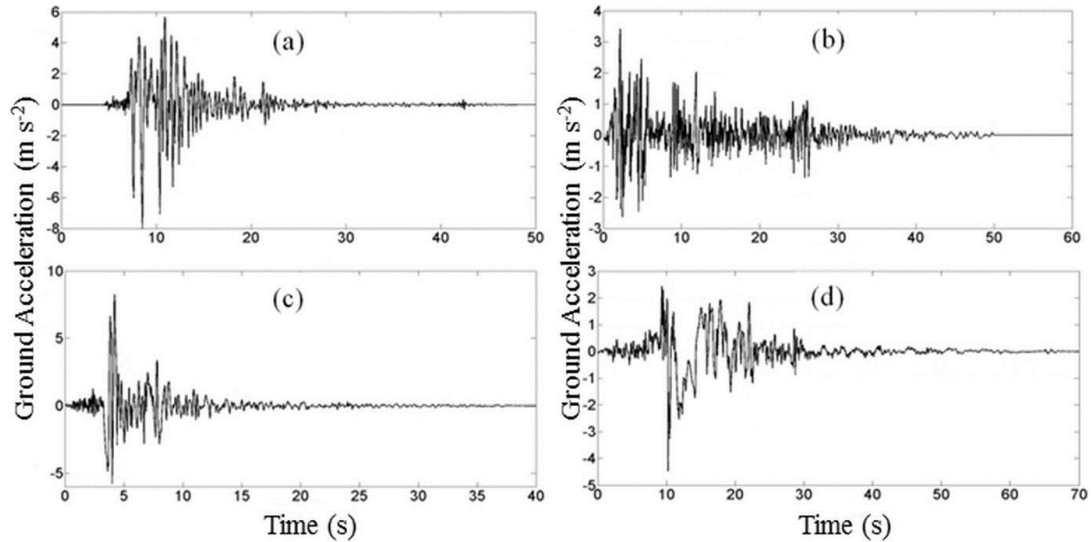

Fig. 2. Acceleration time histories of (a) Kobe, (b) El-Centro, (c) Northridge, and (d) Chi-Chi earthquakes
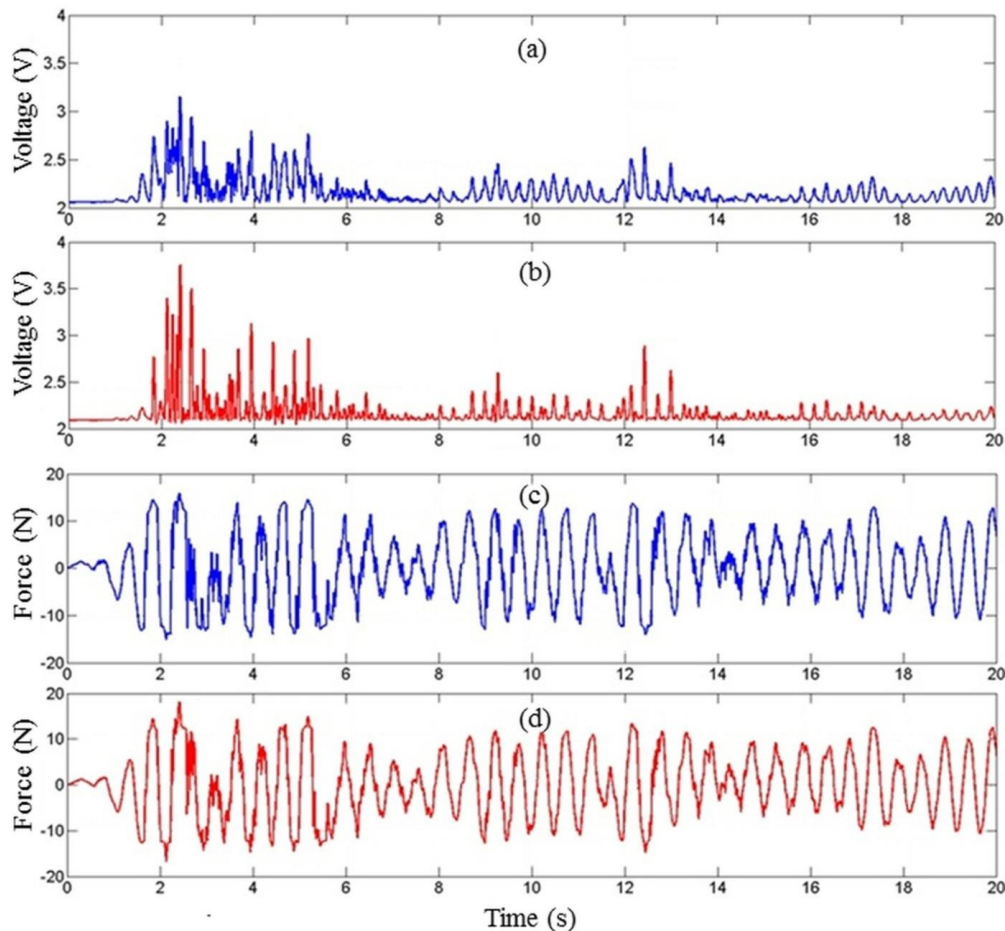

Fig. 3. Time histories of the commanded voltages to dampers of (a) storey 1 and (b) storey 2 and their generated forces for (c) storey 1 and (d) storey 2 during the scaled El-Centro excitation

353

Figure 4 shows the ANFIS controlled and uncontrolled peak responses on all floors of the building. It can be seen from this figure that most of uncontrolled responses except those for a few of the top floors are due to the first mode shape of the building. The few top floors, additionally, are slightly affected by the other mode shapes as well as the first mode shape. The controller has attenuated peak displacements and peak relative inter-storey drifts in all storeys. It has also kept the peak absolute accelerations in an acceptable order in all floors. By the integrated ANFIS controller, the maximum values of displacements, relative inter-storey drifts, and absolute accelerations are reduced from 13.1 mm, 1.00%, and 1.471 m s^{-2} to 7.8 mm, 0.64%, and 1.059 ms^{-2}, respectively. Also, the value of J_4 and J_5, 0.497, and 0.696, shows the ability of ANFIS to control the averaged relative inter-storey drifts and averaged absolute accelerations, as well as, the mentioned maximum values.

In the study of the rigid failure of buildings, it is important to assess the two important criteria, J_3 and J_6. According to these criteria, the building has had 15.5 and 46.6% reduction in the peak and averaged base shear, respectively. This suggests that the building can experience larger amplitudes than the scaled El-Centro by approximately 18.3% in the intense phase of the earthquake and by 87.3% in the other intervals. Although uncontrolled peak and averaged responses do not necessarily lead to structural failure, they can be considered as limits for the purpose of safer designs.

Table 1 compares the proposed control strategy with an integrated fuzzy logic and genetic algorithm (GAF) controller proposed by Yan et al. (2006) and some other conventional methods (presented in Jansen et al., 2000) in which the dynamics of the dampers are not considered explicitly.

Table 1. Structural response criteria resulted from various control strategies

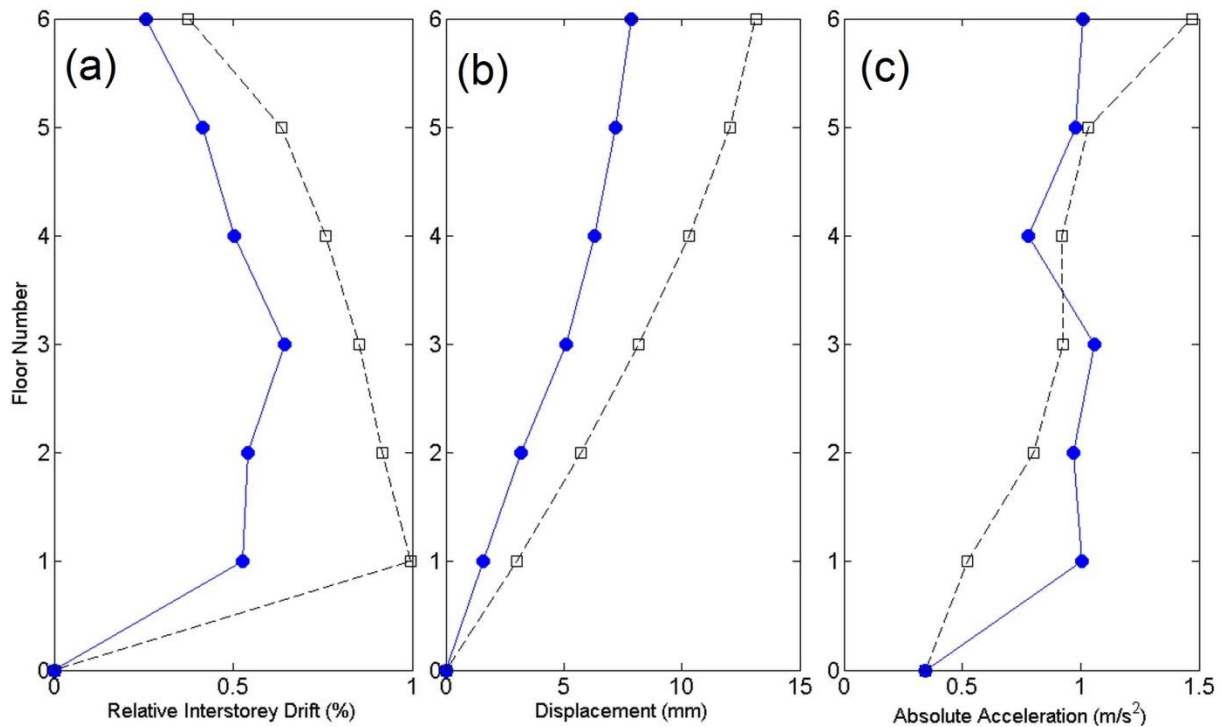| Control Strategy	J_1	J_2	J_7	J_8
Proposed Semi-Active Optimal Strategy	0.646	0.720	0.597	0.0136
GAF	0.630	0.780	0.551	0.0149
Lyapunov Controller A	0.788	0.756	0.686	0.0178
Lyapunov Controller B	0.548	1.39	0.326	0.0178
Decentralized Bang-Bang	0.791	1.00	0.449	0.0178
Maximum Energy Dissipation	0.620	1.06	0.548	0.0121
Clipped-Optimal A	0.640	0.636	0.631	0.01095
Clipped-Optimal B	0.547	1.25	0.405	0.0178
Modulated Homogeneous Friction	0.559	1.06	0.421	0.0178
Passive-Off	0.801	0.904	0.862	0.00292
Passive-On	0.696	1.41	0.506	0.0178

Fig. 4. Peak ANFIS controlled (solid line) and uncontrolled (dashed line) (a) relative inter-storey drift, (b) displacement, and (c) absolute acceleration of all floors during the scaled El-Centro excitation

Table 1 shows that the proposed strategy has been able to better control the J_2 (absolute acceleration) criterion compared to other control strategies. Noting that the control of absolute acceleration is relatively more difficult than the control of displacement and drift, it is interesting that the proposed control algorithm has been able to considerably reduce the maximum relative drift and displacement as well. To explain the lesser success of the control algorithm compared to some of other control strategies, it must be emphasized that when acceleration is the aim of the control strategy, the displacement is not controlled sufficiently and vice versa. The maximum required damper force is 1.36% of the total mass. This is relatively less than the forces used in other control strategies, that is, the proposed algorithm has been able to reduce the absolute acceleration, while using less energy. The proposed strategy has almost the same performance as GAF and Clipped-Optimal A on J_1, J_2, and J_7, but by using less energy.

To show the effectiveness of trained ANFISs in control of other non-trained earthquakes, it has also been applied for Kobe, Northridge, and Chi-Chi excitations, and as the result of other control strategies were not available, they are compared to Passive-on and Passive-off situations. For a meaningful comparison, all earthquakes were scaled to the same PGA as 10% of the El-Centro, 0.3422 ms^{-2}. The results are presented in Figure 5.

Figure 5 shows that the proposed strategy provides better control, on an average, on j_1, j_2, j_3 and j_7 compared to passive-off and passive-on. Moreover, the maximums in J_1, J_2, J_3, and J_7 are reduced by 32, 50.9, 66.9, and 20.4%, which are better than that of passive-on, respectively. Among all earthquakes, the proposed strategy has better performance in j_1 and j_3. Among all earthquakes, except for the Northridge earthquake, it has a better control on J_2. For displacement control, j_7, the proposed strategy shows a better performance for all earthquakes, except for El-Centro.
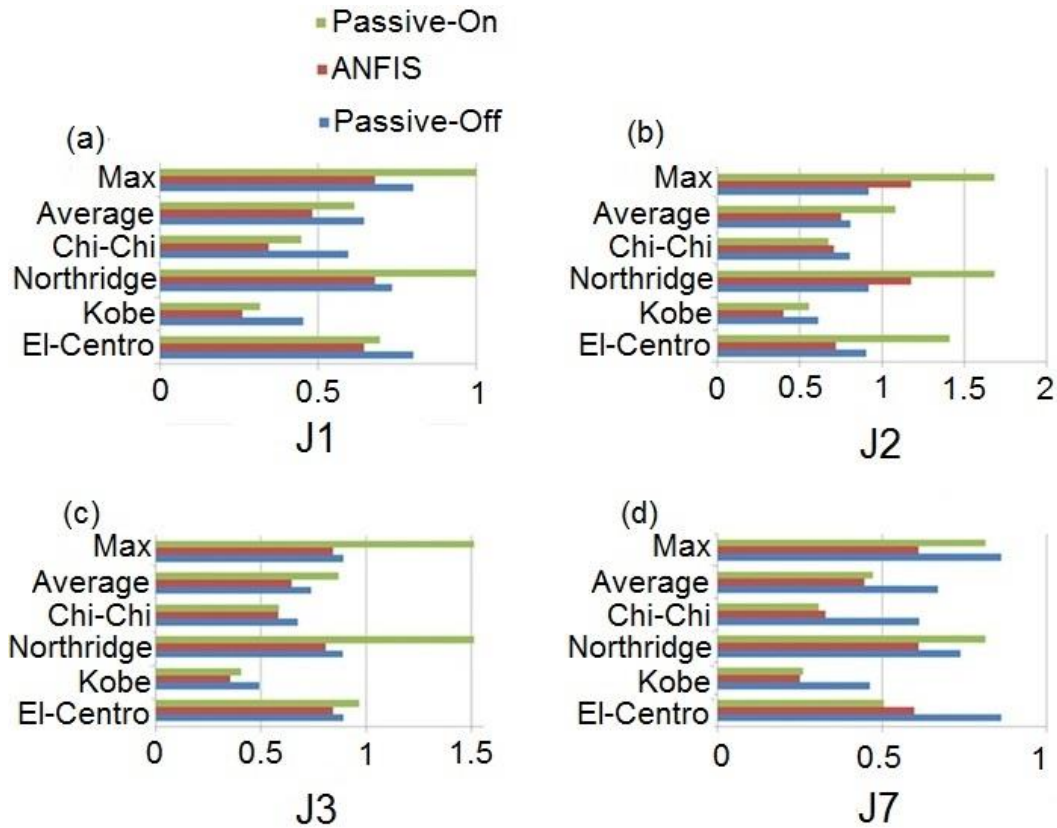
Fig. 5. Results of control by passive-on, ANFIS and passive-off in terms of (a) J_1, (b) J_2, (c) J_3, and (d) J_7 under four earthquakes and their average and maximum

CONCLUSION

In this article a new formulation for optimal control of buildings with MR dampers has been proposed and implemented. The new formulation explicitly integrates the equations of the dynamics of MR dampers with the necessary conditions of optimal control and solves them together. This gives more realistic results than the other conventional algorithms that use a separate *control law*. The outcomes of this formulation are the accurate optimal voltages that are used for training of integrated ANFISs with only absolute acceleration inputs. In this study, a new objective function was also introduced, which includes time-averaged relative inter-storey drifts, absolute accelerations, base shear, and input voltages. Outcomes of control of a building with the proposed method, under a scaled El-Centro excitation, show that it results in better performance compared to the conventional methods.

Also, while the proposed strategy considers the time-averaged J_4, J_5, and J_6 criteria for optimality, its effectiveness is comparable to the GAF and Clipped-Optimal methodsthat consider the J_1, J_2, and J_7 criteria. The proposed strategy reduces the maximum and averaged base shear during the scaled El-Centro earthquake by 15.5 and 46.6%, respectively.

To examine the efficiency of the strategy in control of other earthquakes, the algorithm was applied to the Kobe, Northridge, and Chi-Chi ground excitations, all of which are scaled to the same PGA as the scaled El-Centro. The strategy generally presents better control on J_1, J_2, J_3, and J_7 among the above-mentioned earthquakes than on the passive-on and passive-off. The proposed strategy can effectively reduce displacements, relative inter-storey drifts, absolute accelerations, and the base shear, to a safe level of serviceability, using less force and energy compared to the conventional control strategies.

REFERENCES

Bani-Hani, Kh., Ghaboussi, J. and Schneider, S.P. (1999a). "Experimental study of identification and control of structures using neural network - part1: Identification", *Journal of Earthquake Engineering and Structural Dynamics*, 28(9), 995-1018.

Bani-Hani, Kh., Ghaboussi, J. and Schneider, S.P. (1999b). "Experimental study of identification and control of structures using neural network – part 2: Control", *Journal of Earthquake Engineering and Structural Dynamics*, 28(9), 1019-1039.

Casciati, F., Faravelli, L. and Yao, T. (1996). "Control of nonlinear structures using the fuzzy control approach", *Journal of Nonlinear Dynamics*, 11(2), 171-187.

Chase, J.G., Barroso, L.R. and Hunt, S. (2004). "The impact of total acceleration control for semi-active earthquake hazard mitigation", *Journal of Engineering Structures*, 26(2), 201-209.

Clough, R.W. and Penzin, J. (2003). *Dynamics of structures, 3rd ed.*, Computers & Structures Inc., Berkeley.

Das, D., Datta, T.K. and Madan, A. (2011). "Semiactive fuzzy control of the seismic response of building frames with MR dampers", *Journal of Earthquake Engineering and Structural Dynamics*, 41(1), 99-118.

Dyke, S.J., Spencer, B.F., Sain, M.K. and Carlson, J.D. (1996). "Modeling and control of magneto-rheological dampers for seismic response reduction", *Journal of Smart Materials and Structures*, 5(5), 565-575.

Dyke, S.J. and Spencer, Jr. B.F. (1997). "A comparison of semi-active control strategies for the MR damper", *Proceedings of Intelligent Information Systems*, Grand Bahama Island.

Faruque, A. and Ramaswamy, A. (2009). "Optimal fuzzy logic control for MDOF structural systems using evolutionary algorithms", *Journal of Engineering Applications of Artificial Intelligence*, 22(3), 407-419.

Ghaffarzadeh, H. (2013). "Semi-active structural fuzzy control with MR dampers subjected to near-fault ground motions having forward directivity and fling step", *Journal of Smart Structures and Systems*, 12(6), 595-617.

Jansen, L.M. and Dyke, S.J. (2000). "Semi-active control strategies for MR dampers: Comparative study", *Journal of Engineering Mechanics*, 126(8), 795-803.

Kim, H.S. (2014). "Multi-input multi-output semi-active fuzzy control os seismic-excited building with evolutionary optimization algorithms", *International Journal of Control and Automation,* 7(6), 143-152.

Kirk, D.E. (1970). *Optimal control theory: An introduction*, Prentice Hall Inc., New York.

K-Karamodin, A. and H-Kazemi, H. (2010). "Semi-active control of structures using neuro predictive algorithm for MR dampers", *Journal of Structural Control and Health Monitoring*, 17(3), 237-253.

Liem, D.T., Truong, D.Q., Ahn, K.K. (2015). "Hysteresis modeling of magneto-rheological damper using self-tuning Lyapunov-based fuzzy approach", *International Journal of Precision Engineering and Manufacturing*, 16(1), 31-41.

Ohtori, Y., Christenson, R.E. and Spencer, B.F. (2004). "Benchmark control problems for seismically excited nonlinear buildings", *ASCE Journal of Engineering Mechanics*, 130(4), 366-385.

Schurter, K.C. and Roschke, P.N. (2001). "Neuro-fuzzy control of structures using acceleration feedback", *Journal of Smart Materials and Structures*, 10(4), 770-779.

Shirazi, F.A., Mohammadpour, J., Grigoriadis, K.M. and Gangbing, S. (2012). "Identification and control of an MR damper with stiction effect and its application in structural vibration mitigation", *Journal of IEEE: Transactions on Control Systems Technology*, 20(5), 1285-1301.

Xu, Y.L., Qu, W.L. and Ko, J.M. (2000). "Seismic response control of frame structures using magneto-rheological / electro-rheological dampers", *Journal of Earthquake Engineering and Structural Dynamics*, 29(5), 557-575.

Xu, Z.D. and Guo, Y.Q. (2008). "Neuro-fuzzy control strategy for earthquake-excited nonlinear magnetorheological structures", *Journal of Soil Dynamics and Earthquake Engineering*, 28(9), 717-727.

Yan, G. and Zhou, L.L. (2006). "Integrated fuzzy logic and genetic algorithms for multi-objective control of structures using MR dampers", *Journal of Sound and Vibration*, 296(1-2), 368-382.

Yao, J., Xia, X., Miao, Y., Ma, C. (2013). "Semi-active control system for magnetorheological damper based on identification model with fuzzy neural network", *Journal of Vibroengineering*, 15(4), 2012-2021.

Zhang, J. and Roschke, P.N. (1999). "Active control of a tall structure excited by wind", *Journal of Wind Engineering and Industrial Aerodynamics*, 83(1-3), 209-223.